Molecular Therapy
Original Article

Rescue of GSDIII Phenotype with Gene Transfer Requires Liver- and Muscle-Targeted GDE Expression

Patrice Vidal,[1,2] Serena Pagliarani,[3] Pasqualina Colella,[1,4] Helena Costa Verdera,[1,2] Louisa Jauze,[1,4] Monika Gjorgjieva,[9] Francesco Puzzo,[1,4] Solenne Marmier,[2] Fanny Collaud,[1,4] Marcelo Simon Sola,[1,2] Severine Charles,[1,4] Sabrina Lucchiari,[3] Laetitia van Wittenberghe,[4] Alban Vignaud,[4] Bernard Gjata,[4] Isabelle Richard,[1,4] Pascal Laforet,[5,6,7] Edoardo Malfatti,[5] Gilles Mithieux,[8,9] Fabienne Rajas,[8,9] Giacomo Pietro Comi,[3] Giuseppe Ronzitti,[1,4] and Federico Mingozzi[1,2,4]

[1]INTEGRARE, Genethon, Inserm, Univ Evry, Université Paris-Saclay, 91002 Evry, France; [2]University Pierre and Marie Curie Paris 6 and INSERM U974, Paris, France; [3]Dino Ferrari Centre, Neuroscience Section, Department of Pathophysiology and Transplantation (DEPT), University of Milan, Neurology Unit, IRCCS Foundation Ca' Granda Ospedale Maggiore Policlinico, 20122 Milan, Italy; [4]Genethon, 91002 Evry, France; [5]Myology Institute, Neuromuscular Morphology Unit, Groupe Hospitalier Universitaire La Pitié-Salpêtrière, Sorbonne Universités UPMC Univ Paris 06, 75005 Paris, France; [6]Paris-Est neuromuscular center, Pitié-Salpêtrière Hospital, APHP, 75005 Paris, France; [7]Raymond Poincaré Teaching Hospital, APHP, 92380 Garches, France; [8]Institut National de la Santé et de la Recherche Médicale, U1213, Lyon 69008, France; [9]Université Lyon 1, Villeurbanne 69622, France

Glycogen storage disease type III (GSDIII) is an autosomal recessive disorder caused by a deficiency of glycogen-debranching enzyme (GDE), which results in profound liver metabolism impairment and muscle weakness. To date, no cure is available for GSDIII and current treatments are mostly based on diet. Here we describe the development of a mouse model of GSDIII, which faithfully recapitulates the main features of the human condition. We used this model to develop and test novel therapies based on adeno-associated virus (AAV) vector-mediated gene transfer. First, we showed that overexpression of the lysosomal enzyme alpha-acid glucosidase (GAA) with an AAV vector led to a decrease in liver glycogen content but failed to reverse the disease phenotype. Using dual overlapping AAV vectors expressing the GDE transgene in muscle, we showed functional rescue with no impact on glucose metabolism. Liver expression of GDE, conversely, had a direct impact on blood glucose levels. These results provide proof of concept of correction of GSDIII with AAV vectors, and they indicate that restoration of the enzyme deficiency in muscle and liver is necessary to address both the metabolic and neuromuscular manifestations of the disease.

INTRODUCTION

Glycogen storage disease type III (GSDIII) is a rare (incidence of 1 in 100,000 at birth)[1] autosomal recessive disorder caused by mutations in the *Agl* gene encoding for the glycogen-debranching enzyme (GDE or amylo-alpha-1,6-glucosidase, ExPASy: EC 3.2.1.33, UniProt: P35573). GDE is an enzyme with two catalytic sites involved in the conversion of cytosolic glycogen to glucose.[2]

The clinical manifestations of GSDIII are characterized by two phases: during childhood, the disease has mainly the features of a metabolic disorder with hepatomegaly and severe fasting hypoglycemia, hyperlipidemia, and hyperketonemia; and during adolescence and adulthood, a progressive debilitating myopathy, with a heterogeneous involvement of different muscle groups and exercise intolerance, appears, rendering the metabolic impairment less prominent.[2] GSDIII disease burden is important especially in patients who experience severe skeletal muscle weakness and exercise intolerance.[1,2] Histological analysis of muscle biopsies from GSDIII patients confirms the muscle involvement, and it shows the accumulation of glycogen in large vacuoles that disrupt the myofibrils architecture.[3] Additionally, most GSDIII patients have a cardiac involvement, although only a small percentage (15%) of them develops cardiomyopathy.[2] Additionally, liver complications, such as cirrhosis, development of hepatocellular adenomas (HCAs), and hepatocellular carcinomas (HCCs), have been described in a significant proportion of adult GSDIII patients.[2]

To date, the only therapeutic approach available for GSDIII is symptomatic.[2,4] During childhood, to avoid recurrent hypoglycemia, patients follow a strict diet regimen with frequent meals

Received 28 June 2017; accepted 20 December 2017;
https://doi.org/10.1016/j.ymthe.2017.12.019.

Correspondence: Federico Mingozzi, PhD, Genethon, 1 rue de l'Internationale, 91000 Evry, France.
E-mail: fmingozzi@genethon.fr
Correspondence: Giuseppe Ronzitti, PhD, Genethon, Immunology and Liver Gene Transfer, 1 rue de l'Internationale, 91000 Evry, France.
E-mail: gronzitti@genethon.fr

rich in complex carbohydrates, typically uncooked cornstarch.[5] High-protein high-fat diet has been proposed for adult GSDIII patients, and a strict ketogenic regimen has been reported to be efficacious in preventing hypertrophic cardiomyopathy.[6,7] At present, no therapy has been proposed to address the muscle impairment observed in GSDIII, thus the disease remains an unmet medical need.

The monogenic nature of GSDIII and the fact that it is caused by a well-defined enzyme deficiency make the disease a possible target for gene replacement therapies. To this aim, adeno-associated virus (AAV) vectors represent the platform of choice for *in vivo* gene transfer.[8] Data obtained in the context of clinical trials for hemophilia,[9] congenital blindness,[10] and spinal muscular atrophy[11] demonstrate the safety and therapeutic potential of the AAV vector gene transfer platform. Furthermore, the experience accumulated in large animal models of neuromuscular disorders indicates that systemic administration of AAV vectors results in efficient muscle targeting.[12,13] While promising, one of the most important restrictions in the use of AAV vectors is the size of the transgene expression cassette, which is limited to ~5 kb. Consequently, due to the large size of the GDE cDNA, ~4.6 kb, the development of AAV vector-based strategies for GSDIII is challenging.

Here we describe a new murine model of GSDIII, which faithfully recapitulates the human condition, including body-wide glycogen accumulation, low blood glucose levels, and muscle weakness. Using this model, we tested different gene therapy-based approaches aimed at correcting the disease. Specifically, we showed that overexpression of the lysosomal enzyme alpha-acid glucosidase (GAA) with AAV vectors was not sufficient to fully rescue the GSDIII phenotype *in vivo*. Conversely, using dual overlapping AAV vectors,[14–16] we showed restoration of the GDE enzyme in both liver and muscle, thus demonstrating that the expression of the endogenous enzyme in those tissues is required to clear cytosolic glycogen, rescue muscle strength, and ameliorate blood glucose levels in treated animals. The work presented here provides the framework for the future development of gene therapy approaches for GSDIII.

RESULTS

Development of a Murine Model of GSDIII that Fully Recapitulates the Human Condition

A mouse model of GSDIII ($Agl^{tm1b(EUCOMM)Wtsi}$) was acquired through the International Mouse Phenotyping Consortium (http://www.mousephenotype.org/about-ikmc/eucomm).

The 3-month-old GDE knockout ($Agl^{-/-}$) mice completely lacked GDE expression in liver and skeletal muscle as determined by western blot (Figure 1A) and GDE activity measurement in liver and quadriceps (Figure 1B). As expected, the lack of the enzyme was associated with the accumulation of glycogen in liver, heart, different skeletal muscle groups, and brain (Figure 1C). Additionally, the block of glycogen degradation in the liver led to a dramatic decrease of glucose-6-phosphate levels in $Agl^{-/-}$ animals (Figure 1D).

Detailed histological analysis confirmed the accumulation of glycogen in muscle (Figure S1). Interestingly, the accumulation of glycogen was not homogeneous in all fibers, as some showed comparable glycogen content to that observed in muscle from wild-type littermates ($Agl^{+/+}$ mice; Figure S2). H&E revealed the presence of large vacuoles in muscle fibers that appeared to contain periodic acid Schiff (PAS)-positive material (Figures 1E, 1F, and S1). The presence of vacuoles filled with glycogen strongly resembled the pattern of glycogen accumulation encountered in muscle biopsies from GSDIII patients.[3] Electron microscopy studies on quadriceps from $Agl^{-/-}$ animals disclosed the presence of large glycogen pools disrupting the myofibrillar structure, both in transversal and longitudinal ultrathin sections (Figures 1G and 1H). Higher magnification of the transversal section revealed the presence of small areas containing apparently normally structured glycogen granules that misplaced the myofibrils (Figure 1I), leading to progressive sarcomeric degeneration.

Perhaps one of the most evident phenotypes in young GSDIII patients is the relatively severe and persistent hypoglycemia.[1,4] Accordingly, 6-month-old $Agl^{-/-}$ mice showed a significant reduction in blood glucose levels (Figure 2A) accompanied by an ~3-fold increase in the liver/body weight ratio (Figure 2B), consistent with hepatomegaly and similar to what has been described in GSDIII patients.[1,2] Interestingly, we observed a general decrease in the weight of $Agl^{-/-}$ mice measured at 9 and 12 months of age (Figure S3) that was, however, statistically significant only in females at 12 months of age ($p = 0.046$). Survival, monitored in animals up to 18 months of age, was not impaired in $Agl^{-/-}$ mice ($n = 7$ males, 8 females up to 18 months; $n = 9$ males, 9 females up to 12 months; data not shown). We then evaluated muscle function in affected animals at 3, 6, and 9 months of age. No differences were observed in total distance traveled and rotarod performance (Figures 2C and 2D; Table S1), indicating that glycogen accumulation in muscle and hypoglycemia did not affect general locomotion in $Agl^{-/-}$ mice. Interestingly, when the same mice were tested for muscle strength, we observed a significant ($p = 0.006$) ~20% reduction in grip strength and a profound impairment ($p = 2.2 \times 10^{-7}$) in the wire hang test performance (Figures 2E and 2F, respectively). Functional testing repeated in 6- and 9-month-old animals showed similar results (Table S1).

These results confirm that the model used in this study faithfully recapitulates the human phenotype and, therefore, is suitable to test novel therapeutic strategies to treat GSDIII.

High Levels of GAA Secreted in the Bloodstream Decrease Glycogen Accumulation in Liver but Not in Muscle

GAA is the enzyme responsible for lysosomal glycogen degradation. The lack of this enzyme leads to the accumulation of lysosomal glycogen associated with Pompe disease.[17] Previous results obtained *in vitro* suggest that supraphysiological GAA activity clears glycogen

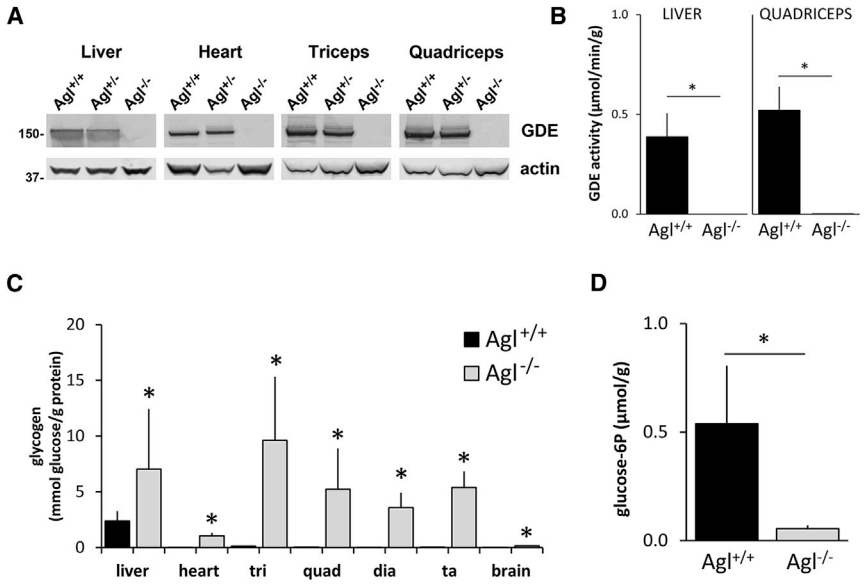

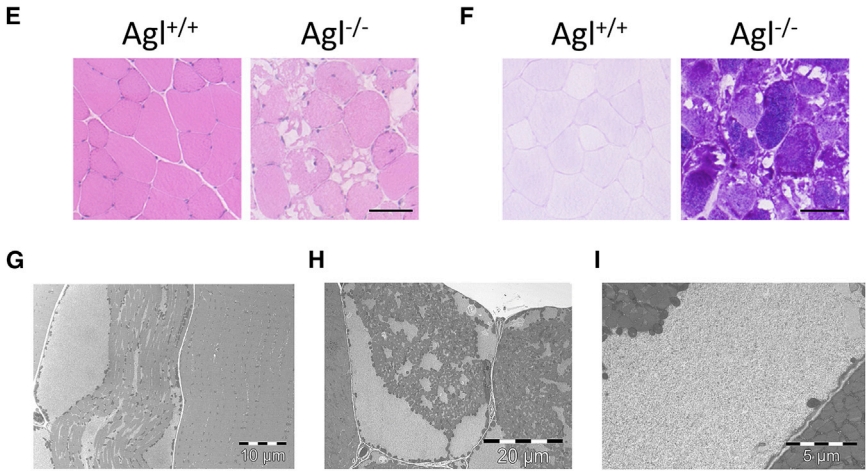

Figure 1. Biochemical and Histological Characterization of Agl$^{-/-}$ Mice

Analysis was performed in 3-month-old male knockout (Agl$^{-/-}$), wild-type (Agl$^{+/+}$), or heterozygous (Agl$^{+/-}$) littermates. (A) Western blot analysis performed in liver, heart, triceps, and quadriceps. An anti-actin antibody was used as a loading control. The positions of molecular weight markers are indicated on the left. (B) GDE activity measured in liver and quadriceps. (C) Glycogen content in liver, heart, triceps and quadriceps, diaphragm, tibialis anterior, and brain reported as mmol of glucose released by complete enzymatic glycogen digestion per gram of protein. (D) Glucose-6-phosphate measured in liver. All data are shown as mean ± SD. Statistical analyses were performed by ANOVA (*$p < 0.05$ versus Agl$^{+/+}$ animals; $n = 5$). (E and F) Representative images of H&E (E) and (F) periodic acid Schiff staining of mouse quadriceps. Scale bars, 50 µm. (G and H) Electron microscopy microphotographs showing, respectively, the longitudinal (G) and the transversal structures (H) of quadricep muscle fibers of a 3-month-old Agl$^{-/-}$ mouse. (I) Higher magnification showing a large vacuole constituted of normally structured glycogen granules.

from primary human GSDIII myoblasts.[18] To test whether GAA overexpression has the potential to rescue glycogen accumulation in GSDIII mice, we took advantage of a recently developed AAV8 vector expressing a secreted form of GAA (AAV-GAA).[19] The 3-month-old GSDIII mice were treated with an AAV-GAA vector at 1×10^{11} or 1×10^{12} vector genomes (vg)/mouse and followed up for 3 months (Figure 3A). As expected, the injection of the AAV-GAA vector resulted in a dose-dependent increase of GAA activity in the bloodstream (Figure 3B) and in supraphysiological levels of GAA enzyme activity in all tissues (Figure 3C, measured at sacrifice).

Interestingly, the administration of the AAV-GAA vector significantly decreased glycogen accumulation in the liver of Agl$^{-/-}$ mice, at both 1×10^{11} and 1×10^{12} vg/mouse ($p = 0.00025$ and 2.7×10^{-6} versus Agl$^{-/-}$ animals, respectively), to levels comparable to those observed in wild-type littermates ($p = 0.092$ and 0.639 versus Agl$^{+/+}$, for the low and high vector dose, respectively; Figure 3D). However, this did not lead to a significant improvement in blood glucose or hepatomegaly (Figure S4). Treatment with AAV-GAA had no effect on glycogen accumulation in Agl$^{-/-}$ muscle (Figure 3D). Accordingly, grip strength and wire hang performance measured 3 months after gene transfer were not rescued in mice treated with AAV-GAA (Figure 3E; Table S2). Interestingly, 1 month post-injection we observed a transient, significant reduction in the number of falls per minute in the wire hang test in animals treated with the AAV-GAA vector at the highest dose ($p = 0.008$ versus untreated Agl$^{-/-}$). No improvement in grip strength was observed at any time point (Table S2).

Together these results indicate that, although high levels of GAA enzyme activity resulted in a decreased glycogen accumulation in the liver, they failed to rescue glycemia and muscle function in GSDIII mice.

Dual Overlapping Vectors Expressing GDE Efficiently Rescue Glycogen Accumulation in the Muscle of GSDIII Mice

Dual overlapping AAV vectors have been used to express genes larger than 5 kb in muscle.[13,14,20] We therefore developed a dual AAV vector expressing the GDE transgene in which the 5′ portion (nucleotides 1–2,688) of the human GDE (hGDE) cDNA was fused with the cytomegalovirus (CMV) promoter and second intron of human beta

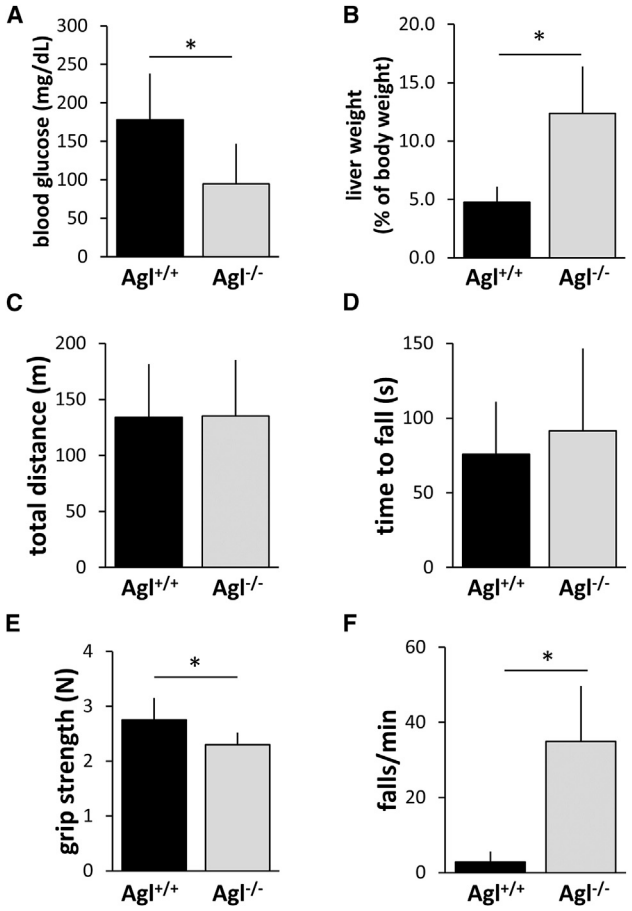

Figure 2. Phenotypic Characterization of Agl$^{-/-}$ Mice

(A) Glycemia measured in 6-month-old male Agl$^{-/-}$ mice and wild-type littermates. Statistical analysis was performed by ANOVA (*$p < 0.05$; n = 23 Agl$^{+/+}$, 52 Agl$^{-/-}$). (B) Liver weight expressed as a percentage of body weight measured in 6-month-old Agl$^{-/-}$ mice and wild-type littermates. Statistical analysis was performed by ANOVA (*$p < 0.05$; n = 14 Agl$^{+/+}$, 16 Agl$^{-/-}$). (C–F) Functional characterization of the muscle strength in 3-month-old Agl$^{-/-}$ male mice and wild-type (Agl$^{+/+}$) littermates. (C) Total distance traveled in 90 min. (D) Time spent on rotarod. (E) Grip strength expressed as the average of three independent measurements. (F) Wire hang test shown as number of falls per minute. Statistical analyses were performed by ANOVA (*$p < 0.05$ versus Agl$^{+/+}$ animals; n = 13 Agl$^{+/+}$, n = 9 Agl$^{-/-}$). All data are shown as mean ± SD.

globin (HBB2)[21] (GDE-HEAD; Figure 4A). The 3′ portion (nucleotides 1,693–4,599) of the hGDE coding sequence was fused with a polyadenylation signal derived from HBB2 (GDE-TAIL; Figure 4A). A region of overlap of 996 nucleotides (nucleotides 1,693–2,688 of the GDE cDNA) was used to mediate the homologous recombination of GDE-HEAD and GDE-TAIL vectors. The two overlapping cassettes were pseudotyped[22] into an AAV9 vector and co-injected in Agl$^{-/-}$ mice at a dose of 1×10^{12} vg/mouse each (Figure 4B). At 3 months after vector injection, most of the vector genomes were found in the liver and heart, whereas quadriceps and triceps had the lowest vector genome copy number (Figure S5). However, while western blot analysis revealed GDE protein expression in heart and skeletal muscles, no protein was detectable in the liver (Figure 4C). Similarly, hGDE transgene mRNA expression levels, normalized for vector genome copy number, were 50- to 800-fold lower in the liver compared to muscle (Figure 4D), suggesting that CMV promoter inactivation in the liver occurred.[23] Accordingly, the absence of expression of the GDE transgene in the liver was associated with a lack of correction of glycemia or hepatomegaly (Figures S6A and S6B).

AAV vector treatment resulted in a significant decrease in glycogen accumulation in several muscle groups, but not in the liver (Figure 4E). In the heart and quadriceps, we observed an inverse correlation ($R^2 = 0.9$ and 0.97, respectively) between the quantity of GDE protein expressed and the glycogen accumulated in the tissue (Figures 4F and 4G). Accordingly, the levels of expression of GDE necessary to clear 80% of glycogen could be estimated to be 8% in the heart and 2% in the quadriceps.

PAS staining confirmed the robust reduction in glycogen accumulation in all muscle groups analyzed, accompanied by a general rescue of the fiber structure as highlighted by H&E staining (Figure 5). Muscle function was also evaluated by monthly measurement of wire hang performance and grip strength. In agreement with the biochemical and histological data, the administration of the dual AAV vector expressing GDE significantly rescued wire hang performance to levels indistinguishable to those measured in wild-type animals ($p = 0.934$ and 0.836 versus Agl$^{+/+}$ at 2 and 3 months post-treatment, respectively; Figure 6A; Table S3). Additionally, a significant improvement in the grip strength was observed in Agl$^{-/-}$ mice treated with overlapping vectors 3 months after the injection ($p = 0.026$ versus Agl$^{-/-}$; Figure 6B; Table S3).

These results indicate that CMV-driven GDE transgene expression mediated by overlapping AAV vectors can rescue the muscle phenotype in GSDIII mice. However, the approach has no effect on the liver manifestations of the disease.

Hepatocyte-Restricted GDE Expression Improves Glycemia in GSDIII Mice

We then tested the dual vector approach by expressing GDE under the transcriptional control of a potent liver-specific promoter.[24] For this experiment, vectors were pseudotyped into AAV8, a capsid that efficiently targets the liver in mice.[25] The injection of Agl$^{-/-}$ mice with the combination of the overlapping vectors (GDE-HEAD with the liver-specific promoter and GDE-TAIL, each of them at the dose of 1×10^{12} vg/mouse), resulted in detectable expression of GDE protein in the liver of 5/8 AAV-treated mice, measured by western blot (Figure 7A). Glycogen accumulation in the liver of Agl$^{-/-}$ animals treated with the dual AAV vector was indistinguishable from that measured in wild-type Agl$^{+/+}$ animals ($p = 0.409$; Figure 7B). Accordingly, we observed a significant improvement of the blood glucose in treated Agl$^{-/-}$ mice at all time points tested ($p = 0.0008$ versus untreated Agl$^{-/-}$, two-way

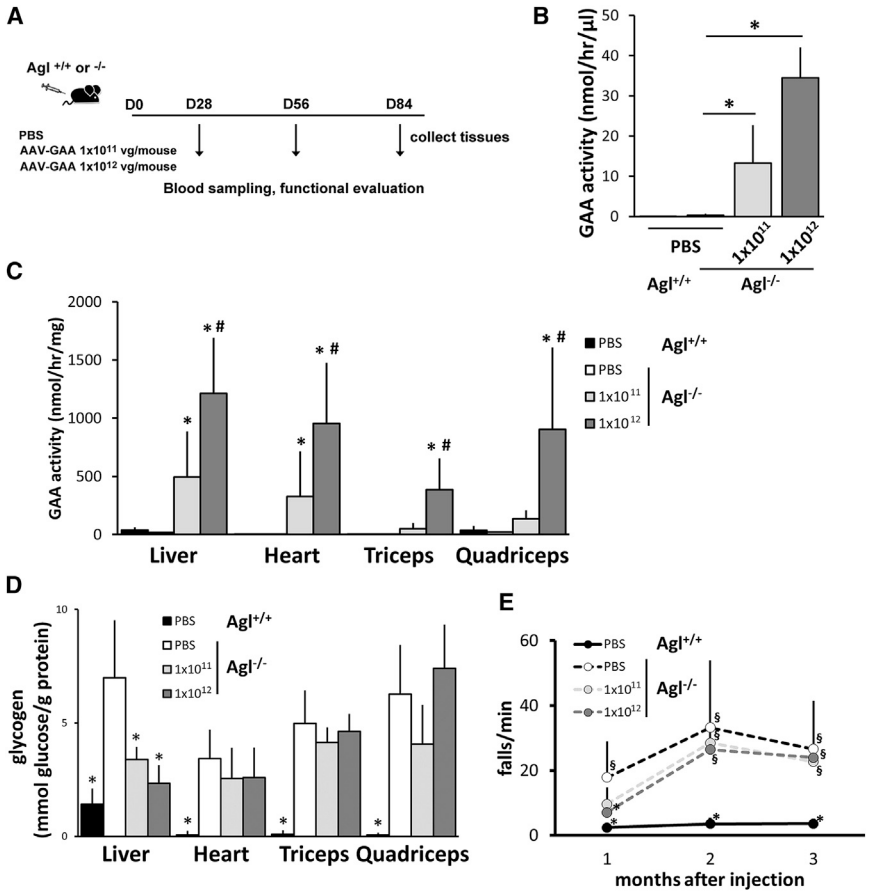

Figure 3. AAV-Mediated GAA Overexpression Rescues Glycogen Accumulation in the Liver of Agl$^{-/-}$ Mice

(A) 3-month-old Agl$^{-/-}$ mice were injected intravenously with PBS or with 1 × 10^{11} or 1 × 10^{12} vg/mouse of a vector expressing secretable GAA. Wild-type littermates (Agl$^{+/+}$) injected with PBS served as the controls. Injected mice were bled and functionally tested at days 28, 56, and 84 and sacrificed 3 months after injection. (B) GAA activity measured in serum 3 months post-injection. (C) GAA activity measured at sacrifice in liver, heart, triceps, and quadriceps. (D) Glycogen content in liver, heart, triceps, and quadriceps measured at sacrifice and reported as mmol of glucose released by complete enzymatic digestion per gram of protein. (E) Wire hang test performed 1, 2, and 3 months post-injection. Statistical analyses were performed by ANOVA (*p < 0.05 versus PBS injected Agl$^{-/-}$, #p < 0.05 versus 1 × 10^{11} AAV-GAA injected mice, §p < 0.05 versus PBS injected Agl$^{+/+}$; n = 7–11 mice/group). All data are shown as mean ± SD.

ANOVA time × treatment; Figure 7C). Despite the positive impact on glycogen accumulation and glycemia, AAV gene transfer was not able to correct hepatomegaly (Figure S7). To evaluate the correlation between GDE expression and liver phenotype correction, we stratified the analysis by dividing samples in two different groups based on GDE expression as measured by western blot, the group HIGH expressing GDE and the group LOW showing no expression of the protein. We observed a 4-fold difference in GDE mRNA expression between the two groups (Figure S8A). Interestingly, we observed a better correction of glycemia, hepatomegaly, and glycogen accumulation in animals of the group HIGH (Figures S8B–S8D).

These results demonstrate that efficient liver expression of GDE rescues glycemia, glycogen accumulation, and hepatomegaly.

Impact of Gene Transfer on Liver Metabolism in GSDIII Mice

Based on the results obtained with gene transfer *in vivo*, we sought to compare the effect of GAA and GDE gene transfer on liver metabolic pathways. To this aim, we analyzed the levels of expression of a panel of genes involved in different pathways of the mouse glucose and glycogen metabolism (Figures 8A and 8B). The level of expression of 76 genes expressed in the mouse liver was analyzed. When compared to wild-type Agl$^{+/+}$ animals, untreated Agl$^{-/-}$ mice showed, with some exception, a generalized downregulation of all the pathways investigated (Figures 8C and 8D). 43 genes were significantly changed in at least one of the three groups analyzed (untreated Agl$^{-/-}$, AAV-GAA, and AAV-GDE overlapping treated Agl$^{-/-}$; p < 0.05 by ANOVA). Of these 43 genes, only 19 showed an n-fold > ± 1.75 (Table S4), and 11 genes were changed in untreated Agl$^{-/-}$ mice; 4/11 genes were rescued in animals treated with AAV-GAA vector, whereas the treatment with overlapping AAV vectors expressing GDE rescued 8/11 genes (Table S4). A general tendency to the normalization of all the genes modified in Agl$^{-/-}$ animals could be observed after treatment with GDE-expressing vectors, but not in AAV-GAA-treated animals' vectors, as shown by heatmap analysis (Figures 8E and 8F).

These results suggest that GDE expression in the liver mediates a better control of glucose metabolism than GAA overexpression.

Simultaneous Liver and Muscle Gene Transfer Corrects Liver and Muscle Phenotype in Agl$^{-/-}$ Mice

Next, we evaluated the possibility to correct the disease phenotype in liver and muscle by using a strong, constitutive promoter, active in liver. Dual overlapping vectors expressing GDE under the transcriptional control of the CMV enhancer chicken beta-actin promoter (CAG) were pseudotyped in AAV9. The 3-month-old Agl$^{-/-}$ mice were injected with the combination of the overlapping vectors (each of them at the dose of 1 × 10^{12} vg/mouse). At 1 month after vector injection, we observed a partial rescue of glycemia in treated Agl$^{-/-}$ mice (Figure S9A) and a complete rescue of muscle function as measured by wire hang (Figure S9B).These data, although preliminary, seem to

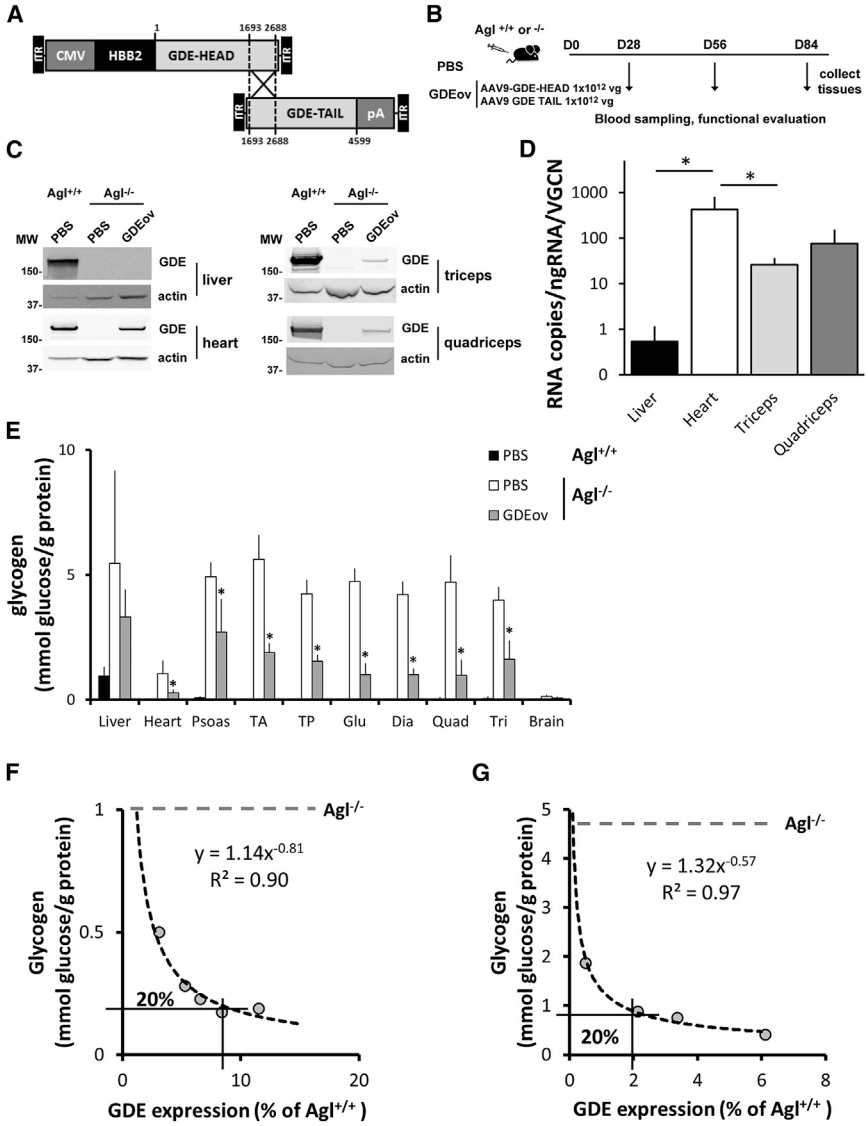

Figure 4. Gene Transfer with a Dual AAV Vector Expressing GDE Rescues Glycogen Accumulation in the Muscle of GSDIII Mice

(A) Schematic representation of the AAV9-GDE-HEAD and AAV9-GDE-TAIL vectors. CMV, cytomegalovirus enhancer/promoter; HBB2, human beta-2 globulin intron; pA, HBB2 polyadenylation signal; ITR, inverted terminal repeats. (B) 3-month-old Agl$^{-/-}$ mice were injected intravenously with PBS or with 2 × 10^{12} vg/mouse of the combination of AAV9-GDE-HEAD and AAV9-GDE-TAIL in a 1:1 ratio (GDEov). As a control, wild-type littermates (Agl$^{+/+}$) were injected intravenously with PBS. Injected mice were bled and functionally tested at days 28, 56, and 84 and sacrificed 3 months after the injection. (C) Western blot analysis for GDE in liver, heart, triceps, and quadriceps. An anti-actin antibody was used as a loading control. MW, molecular weight marker. (D) hGDE mRNA expression normalized per vector genome copy number in liver, heart, triceps, and quadriceps. (E) Glycogen content measured 3 months post-injection and reported as mmol of glucose released by complete enzymatic digestion per gram of protein. Statistical analyses were performed by ANOVA (*$p < 0.05$ versus PBS injected Agl$^{-/-}$). (F and G) Correlation between GDE protein levels expressed as the percentage of GDE in Agl$^{+/+}$ animals and glycogen accumulation in (F) heart and (G) quadriceps of Agl$^{-/-}$ treated with dual AAV vectors. The power regression formula and the regression coefficient (R^2) are depicted. The gray, dotted line indicates glycogen levels in untreated Agl$^{-/-}$ animals, and the black line indicates the level of GDE protein expression necessary to obtain the clearance of 80% of this glycogen (or 20% of residual glycogen). All data are shown as mean ± SD.

indicate that the use of a constitutive promoter active in the liver could rescue both liver and muscle phenotype in Agl$^{-/-}$ mice.

DISCUSSION

GSDIII is a debilitating neuromuscular and metabolic disease with no curative therapeutic options. This exposes young patients to persistent hypoglycemia, which becomes less severe in adulthood when a more pronounced debilitating muscle phenotype appears. The major impact of the disease on the quality of life of patients and the lack of effective treatments besides dietary management prompted us to develop new gene therapy approaches to GSDIII.

Here we describe the development and characterization of a mouse model that faithfully recapitulates the disease phenotype in humans, including low blood glucose, hepatomegaly, whole-body accumulation of glycogen, and muscle weakness. With this model, we tested different treatment modalities based on AAV vector gene transfer.

Based on the observation that there is a small percentage of glycogen continuously trafficking from the cytosol to the lysosome,[26] we tested whether the overexpression of the lysosomal enzyme GAA could rescue the phenotype of GSDIII. To this aim, we used a highly efficient AAV vector expressing GAA, which was recently demonstrated to mediate whole-body treatment of Pompe disease.[19] Despite achieving supraphysiological levels of GAA activity in most tissues, in GSDIII mice this approach had only a limited and transient effect on muscle performance. A significant reduction of glycogen accumulation was only observed in the liver, although no effect on glycemia or hepatomegaly was observed. These results are consistent with data obtained *in vitro* with GSDIII myoblasts treated with recombinant GAA enzyme, in which a partial rescue of glycogen accumulation was observed.[18] Why the effect of GAA on muscle function in GSDIII mice is only transient remains to be assessed. One hypothesis is that, due to the low rate of cytosolic glycogen trafficking to lysosomes in muscle, its pathological accumulation is not fully cleared by GAA overexpression. Based on this, adjuvant therapies aimed at enhancing

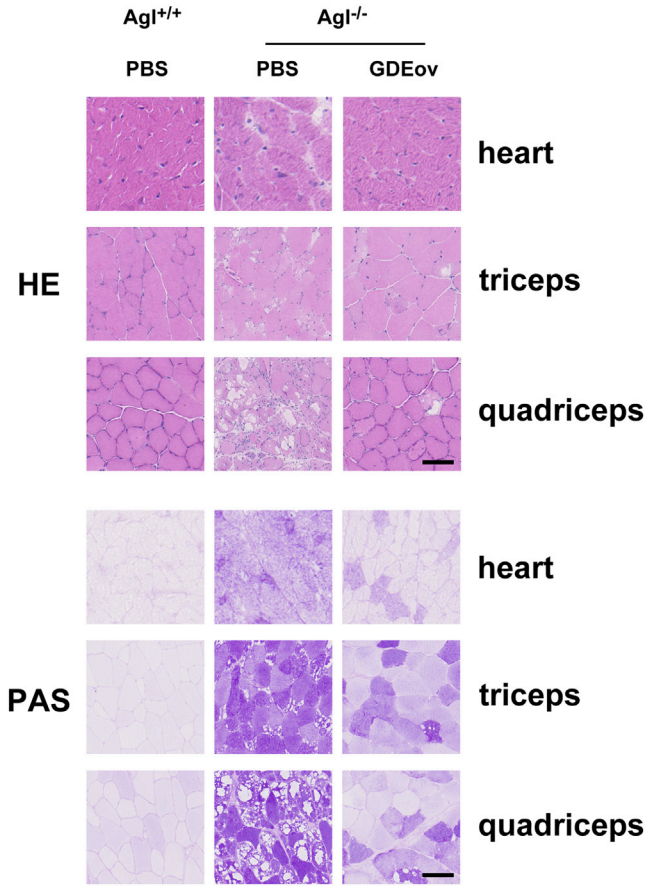

Figure 5. Histological Analysis Confirms Dual AAV Vector-Mediated Rescue of Glycogen Accumulation in the Muscle of Agl$^{-/-}$ Mice

H&E staining (upper panels) and periodic acid Schiff (PAS, lower panels) staining performed in heart, triceps, and quadriceps of 6-month-old mice treated as described in Figure 4. Scale bars, 50 μm.

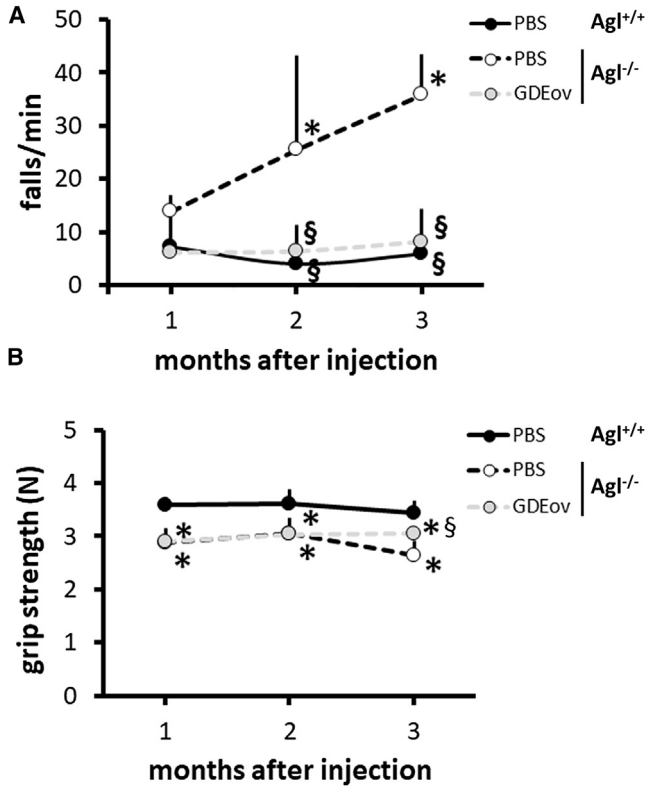

Figure 6. Dual AAV9 Vector Expressing GDE Rescues Muscle Function in GSDIII Mice

Assessment of muscle strength in wild-type and Agl$^{-/-}$ mice treated as described in Figure 4. Functional testing was performed 1, 2, and 3 months post-treatment. (A) Wire hang test shown as number of falls per minute. (B) Grip test expressed as the average of three independent measurements. Statistical analyses were performed by ANOVA (*$p < 0.05$ versus PBS-injected Agl$^{+/+}$, §$p < 0.05$ versus PBS-injected Agl$^{-/-}$, $n = 5$). All data are shown as mean ± SD.

autophagy, e.g., by using rapamycin[27] or in combination with diet,[28–30] may improve the efficacy of this approach in GSDIII. The mechanism(s) underlying the difference in glycogen clearance mediated by GAA in muscle versus liver is also unclear. However, similar observations have been reported after the treatment of GSDIV mice with GAA that resulted in the clearance of liver, but not muscle, glycogen.[31]

Based on the observation that overexpression of GAA alone does not fully correct GSDIII, we sought to address the enzymatic deficiency, hallmark of the disease, by directly restoring the GDE enzyme activity with AAV vectors. The fact that GDE is a large cytosolic protein of 175 kDa with two different enzymatic domains[32] complicates the design of AAV vectors expressing the enzyme, and it does not allow for the development of gene therapy strategies based on cross-correction.[19,33,34]

To overcome this limitation, we developed a dual AAV vector strategy[13,14,20,35] to express GDE transgene in liver and muscle. CMV promoter-driven GDE transgene expression mediated the complete rescue of muscle function and glycogen accumulation in different muscle groups, including the heart.[36] Biochemical parameters correlated with muscle histology and PAS staining, which showed good correction of the disease phenotype. Conversely, due to the silencing of the CMV promoter in liver,[23] no liver GDE expression was detected and no corrections of glycogen accumulation, hepatomegaly, or glycemia were observed, indicating that targeting muscle alone would not rescue the metabolic impairment hallmark of GSDIII.

To address this limitation and to better explore the role of liver pathology in GSDIII, we designed a dual AAV vector expressing the GDE transgene under the control of a liver-specific promoter.[25] With this strategy, treated animals showed improved glycemia and clearance of liver glycogen. No effect of gene transfer on hepatomegaly was observed, perhaps indicating that higher expression levels are needed to fully correct the hepatic phenotype in our model.

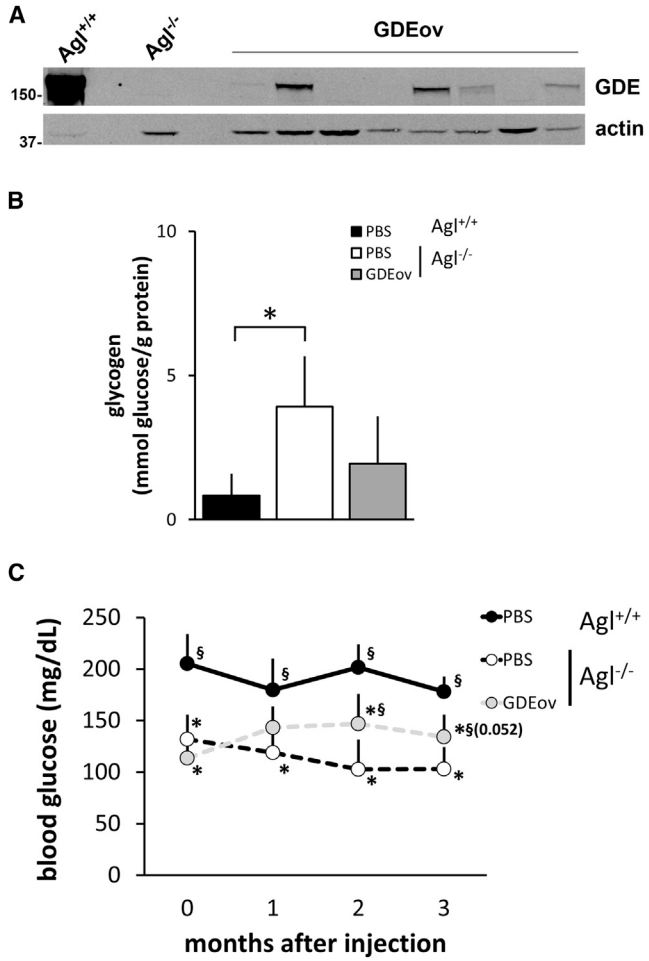

Figure 7. Liver-Specific Expression of GDE with a Dual AAV Vector Rescues Glycemia in GSDIII Mice

3-month-old $Agl^{-/-}$ mice were intravenously injected with PBS or with 2×10^{12} vg/mouse of AAV8-hAAT-GDE-HEAD and AAV8-GDE-TAIL (GDEov) vectors at a 1:1 ratio. Wild-type littermates ($Agl^{+/+}$) were used as controls. (A) Western blot analysis in liver. An anti-actin antibody was used as a loading control. The positions of a molecular weight marker running in parallel with samples are indicated on the left. (B) Glycogen content measured in liver 3 months post-injection and reported as mmol of glucose released by complete enzymatic digestion per gram of protein. Statistical analyses were performed by ANOVA (*$p < 0.05$ versus PBS injected $Agl^{+/+}$). (C) Glycemia measured before and 1, 2, and 3 months post-injection. Statistical analyses were performed by two-way ANOVA time × treatment (*$p < 0.05$ versus PBS injected $Agl^{+/+}$, §$p < 0.05$ versus PBS injected $Agl^{-/-}$; $Agl^{+/+}$ n = 9, $Agl^{-/-}$ n = 4, $Agl^{-/-}$ treated with GDEov n = 8 mice/group). All data are shown as mean ± SD.

Gene expression analysis allowed us to compare the impact of GAA versus GDE gene transfer on glucose metabolism in the liver. In untreated knockout animals versus wild-type controls, the pathways that appeared mostly affected were the regulation of glucose metabolism and the tricarboxylic acid (TCA) cycle. Although results indicate that a general normalization was observed following hepatic GDE gene transfer, the dependency of glucose metabolism on diet, gender, and age represents a major limit of this study. Nevertheless, the fact that GAA gene transfer mediated the rescue of only a limited subset of genes further supports the need for correction of the underlying enzyme defect to rescue the metabolic impairment in GSDIII.

Data presented here provide insights into the disease and its treatment, in particular on the importance of mobilizing cytosolic glycogen in both the liver and muscle to mediate full rescue of the phenotype. The metabolic impairment in GSDIII is particularly important in pediatric patients, where the liver growth could affect the efficacy of AAV-mediated liver gene transfer.[37,38] However, in adult GSDIII patients, liver disease manifestation is associated with the development of HCA and HCC.[39] Thus, the development of effective treatments targeting the liver, in addition to muscle, in adult GSDIII patients is highly needed. CAG promoter seems to be an option to efficiently express GDE both in liver and muscle. However, systemic expression of transgenes has been associated with the development of anti-transgene immune response.[40,41] Thus, future work will be focused on the development of expression cassettes to drive efficient GDE expression specifically in the two tissues.

The approach presented here has some limitations associated with the use of dual AAV vectors, specifically (1) the low efficiency of reconstitution of the full-length transgene cDNA mediated by the overlapping complementary sequence,[15] and (2) the fact that the homologous recombination machinery is not equally efficient in all tissues.[15] Alternative strategies could be used to enhance the efficiency of homologous recombination to reconstitute the full-length transgene expression cassette. These may include dual hybrid AAV carrying transgene-independent highly recombinogenic DNA sequences.[15,16] Additionally, small enhancer elements[42] and synthetic promoters[43] combined with AAV serotypes that efficiently target the muscle[44] could increase expression of the GDE transgene.

Finally, data obtained here provide some estimate on the threshold of GDE transgene expression required to obtain therapeutic efficacy. A nearly full rescue of muscle function was observed in GSDIII mice treated with the dual AAV vector expressing the GDE transgene, despite partial restoration of the enzyme expression. This indicates that only a small increment in enzyme activity is sufficient to dramatically improve the muscle phenotype in GSDIII, in line with the concept that the therapeutic threshold, in terms of vector dose, for muscle enzyme deficiencies is lower than that of muscular dystrophies, in which muscle structural proteins are defective.[45]

Future efforts will have to focus on improving efficiency of GDE expression in the muscle and in the liver to mediate correction of both the muscle and the metabolic impairment hallmarks of GSDIII. As more information about the efficiency of transduction of dual AAV vectors in muscle[14,16,20,46–49] and in other tissues[15,35] emerges

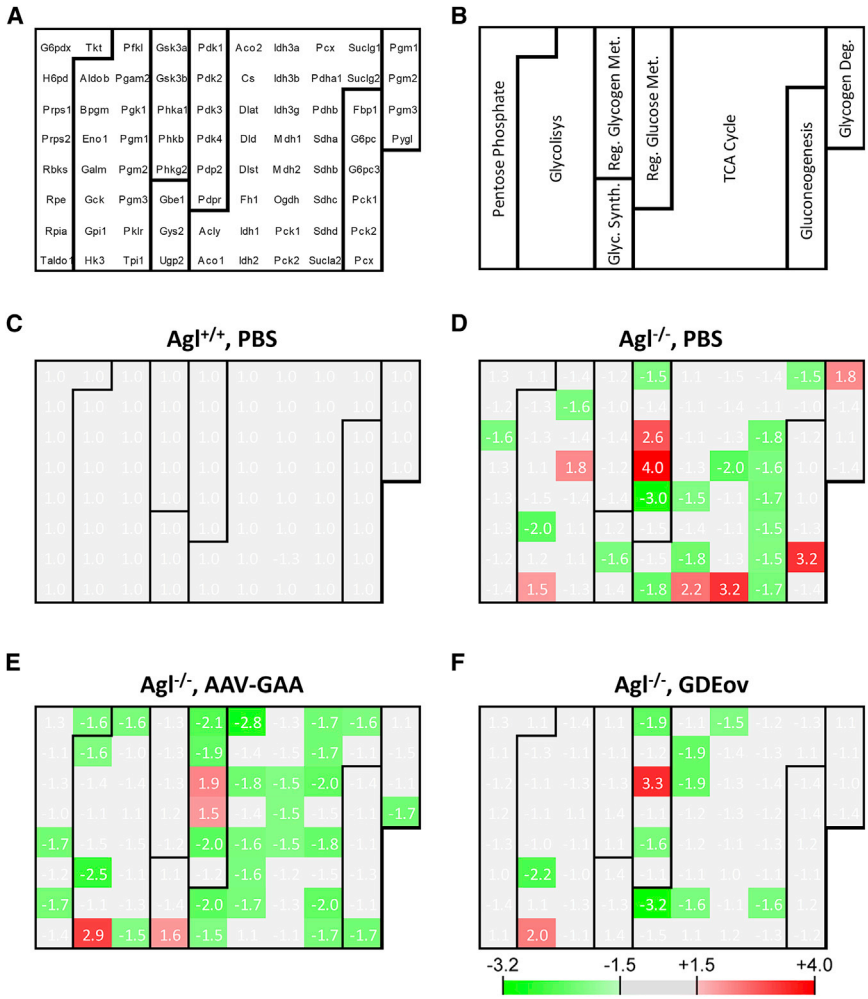

Figure 8. Heatmap Analysis of the Expression Profile of Genes Involved in the Mouse Glucose Metabolism

RNAs were extracted from livers of 6-month-old $Agl^{-/-}$ mice injected intravenously at 3 months of age with PBS, 1×10^{12} vg/mouse of a vector expressing engineered GAA (AAV-GAA), or 2×10^{12} vg/mouse of overlapping AAV vectors expressing GDE in the liver (GDEov). Wild-type littermates injected intravenously with PBS were used as controls. (A) Genes names. (B) Functional role of the genes analyzed. The scheme indicates the regions of the heatmap corresponding to groups of genes involved in specific pathways, namely, pentose phosphate, glycolysis, glycogen synthesis (Glyc. Synth.), regulation of the glycogen metabolism (Reg. Glycogen Met.), regulation of glucose metabolism (Reg. Glucose Met.), citric acid cycle (TCA cycle), gluconeogenesis, and glycogen degradation (Glycogen Deg.). (C–F) Heatmaps indicating the levels of expression of the genes in $Agl^{+/+}$ mice injected with PBS (C) or $Agl^{-/-}$ mice injected with PBS (D), AAV-GAA (E), or GDEov (F) and normalized to levels measured in $Agl^{+/+}$. Colors scale for fold change in expression is indicated at the bottom of the graphs.

from preclinical and clinical studies, critical parameters for the successful translation of dual AAV vectors to the clinic will become evident. Specific safety parameters of dual AAV vectors will also have to be carefully defined, such as the expression of truncated sequences from the single non-annealed AAV carrying the GDE transgene and transgene immunogenicity.

In conclusion, the work presented here provides a demonstration of correction of GSDIII in both liver and muscle *in vivo* with dual AAV vectors. Results obtained help to define the levels of GDE protein expression needed to rescue the disease phenotype, both at the functional and biochemical levels, and they lay the fundaments for future translational efforts toward the development of a curative treatment for the disease.

MATERIALS AND METHODS

In Vivo Studies

The *Agl* knockout ($Agl^{-/-}$) mice were developed in the frame of the International Mouse Phenotyping Consortium (IMPC). Mice were generated in a pure C57BL/6J background by replacing exons 6–10 of the *Agl* gene with a neomycin-expressing cassette. Mice were bred into a mixed BALB/c background for the purpose of this study.

All mouse studies were performed according to the French and European legislation on animal care and experimentation (2010/63/EU) and approved by the local institutional ethical committee (protocol 2016-002). AAV vectors were administered intravenously via the tail vein to 3-month-old male $Agl^{-/-}$ mice and wild-type littermates ($Agl^{+/+}$).

Western Blot Analysis

Mouse tissues were homogeneized in DNase/RNase-free water, and protein concentration was determined using the BCA Protein Assay (Thermo Fisher Scientific, Waltham, MA). SDS-PAGE electrophoresis was performed in a 4%–15% gradient polyacrylamide gel. After transfer, the membrane was blocked with Odyssey buffer (LI-COR Biosciences, Lincoln, NE) and incubated with an anti-GDE antibody (Rabbit polyclonal, AS09-454, Agrisera) and an anti-actin antibody (Rabbit monoclonal, sc-8432, Santa Cruz Biotechnology). The membrane was washed and incubated with the appropriate secondary antibody (LI-COR Biosciences) and visualized by Odyssey imaging system (LI-COR Biosciences).

Enzyme Activity Measurements

GAA activity was measured as previously described.[19] The protein concentration of the samples prior to GAA activity measurement was quantified by BCA (Thermo Fisher Scientific, Waltham, MA).

GAA activity was reported as nmol/hr/mg protein when measured in tissue and as nmol/hr/μL when measured in plasma.

GDE activity was measured as previously described.[50] Briefly, 50 mg tissue was homogeneized in 50 μL DNase/RNase-free water. The lysate was incubated at 37°C with limit dextrin in 4.5 mM EDTA and 0.16 M phosphate buffer (pH 7). The reaction was then centrifuged. Supernatants were used to measure the glucose produced using a glucose assay kit (Sigma-Aldrich, St. Louis, MO) and by measuring resulting absorbance on an EnSpire alpha plate reader (PerkinElmer, Waltham, MA) at 540 nm.

Measurement of Glycogen Content

Glycogen content was measured indirectly in tissue homogenates as the glucose released after total digestion with *Aspergillus Niger* amyloglucosidase (Sigma-Aldrich, St. Louis, MO). Samples were incubated for 5 min at 95°C and then cooled at 4°C; 25 μl amyloglucosidase diluted 1:50 in 0.1 M potassium acetate (pH 5.5) was then added to each sample. A control reaction without amyloglucosidase was prepared for each sample. Both sample and control reactions were incubated at 37°C for 90 min. The reaction was stopped by incubating samples for 5 min at 95°C. The glucose released was determined as described below (see Glycemia Measurement).

Histology and Electron Microscopy

For muscle histology, heart, diaphragm, triceps brachii, quadriceps femoris, tibialis anterior and posterior, gluteus maximus, and psoas were snap-frozen in isopentane previously chilled in liquid nitrogen. Serial 8-μm cross sections were cut in a Leica CM3050 S cryostat (Leica Biosystems, Nussloch, Germany). To minimize sampling error, 3 sections of each specimen were obtained and stained with H&E and PAS according to standard procedures.

Electron microscopic analysis was performed in quadricep muscles from wild-type and $Agl^{-/-}$ animals. Specimens were fixed with glutaraldehyde (2.5%, pH 7.4), postfixed with osmium tetroxide (2%), dehydrated, and embedded in resin (EMBed-812; Electron Microscopy Sciences, Hatfield, PA). Ultrathin sections were stained with uranyl acetate and lead citrate. The grids were observed using an electron microscope (80 kV; Model CM120; Philips Electronics NV, Eindhoven, the Netherlands) and photographed (Morada Soft Imaging System; Olympus France).

Glycemia Measurement

Glycemia was measured using sera collected from mice fed normally. A glucose assay kit (Sigma-Aldrich, St. Louis, MO) was used, and the resulting absorbance was acquired on an EnSpire alpha plate reader (PerkinElmer, Waltham, MA) at a wavelength of 540 nm.

Muscle Function Tests

Forelimb wire hang test was performed as already reported.[19,51] A 4-mm-thick wire was used to record the number of falls over a period of 3 min. The average number of falls per minute was reported for each animal.

Grip strength was measured as already reported.[19,51] Using a grip strength meter (Columbus Instruments, San Diego, CA), three independent measurements of the four limbs' strength were recorded at each time point. Maximum values of the grip strength were reported.

Rotarod testing was performed as already reported[19,52] using an LE8200 apparatus (Harvard Apparatus, Holliston, MA). An accelerating protocol 4–40 rpm in 5 min was used. The test was repeated three times and the best performance of each animal was reported.

Production of AAV Vectors

All AAV vectors used in this study were produced using an adenovirus-free transient transfection method[53] and purified as described earlier.[54] Titers of the AAV vector stocks were determined using a real-time qPCR and confirmed by SDS-PAGE, followed by SYPRO Ruby protein gel stain and band densitometry.

Human GAA Transgene Engineering and Transgene Expression Cassette

The native GAA signal peptide (amino acids 1–27, starting from the ATG) was removed and replaced by chimotrypsinogen B2 signal peptide (UniProt: Q6GPI1). Additionally, amino acids 28–35 of the GAA pro-peptide were removed to generate a truncated version of the transgene. Transgene expression was under the control of the hepatocyte-specific human alpha-1 anti-trypsin (hAAT) promoter, combined with a synthetic human beta-globin-derived (HBB2) intron (32) and bovine growth hormone polyA (bGH). The entire expression cassette was flanked by the inverted terminal repeats of AAV serotype 2 for vector packaging.

Vector Genome Copy Number Determination

Vector genome copy number was determined using a qPCR assay as previously described.[21] The PCR primers used in the reaction were located in the overlapping region of human GDE transgene, forward primer 5′-GTCTTGATAACTGCCACTCA-3′ and reverse primer 5′-AAAGTAACATGGGATAAGGT-3′, for the vector. For the internal control titin gene, the sequences of the forward and reverse primers were 5′-AAAACGAGCAGTGACGTGAGC-3′ and 5′-TTCAGTCATGCTGCTAGCGC-3′, respectively.

Gene Expression Analysis

For GDE transgene expression, total RNA was extracted from cell lysates using Trizol (Thermo Fisher Scientific, Waltham, MA). DNA contaminants were removed using the Free DNA kit (Thermo Fisher Scientific, Waltham, MA). Total RNA was reverse-transcribed using random hexamers and the RevertAid H minus first strand cDNA synthesis kit (Thermo Fisher Scientific, Waltham, MA). qPCR was performed with oligonucleotides specific for the GDE transgene (forward 5′-CTGGAGTTGCCACAAAAGGG-3′ and reverse 5′-AGTGAGG ACTGAATTGTGTC-3′) and normalized by the levels of expression of GAPDH (forward 5′-GTTGTCTCCTGCGACTTCA-3′ and reverse 5′-GGTGGTCCAGGGTTTCTTA-3′).

For the gene expression analysis with RT^2 Profiler PCR Array, a Mouse Glucose Metabolism RT^2 Profiler PCR Array (QIAGEN, Hilden, Germany) was used, following the manufacturer's directions. The array included 89 genes, 5 of which were housekeeping genes used for normalization (beta-actin, beta-2 microglobulin, glyceraldehyde-3-phosphate dehydrogenase, beta glucuronidase, heat shock protein 90 alpha [cytosolic], class B member 1) as indicated by the manufacturer. 14 genes were removed because they were not expressed in mouse liver. The level of expression of the remaining 70 genes was used for the heatmap analysis. Six genes, as indicated by the manufacturer, were assigned to two different functional classes. Genes were sorted based on their role in specific glucose metabolism pathways.

Statistical Analysis

All the data shown in this paper are reported as mean ± SD. The StatistiXL software (StatistiXL, Broadway, Australia) was used for statistical analysis. p values < 0.05 were considered significant. For all the datasets, data were analyzed by parametric tests, alpha = 0.05 (one-way and two-way ANOVA with Tukey's post hoc correction). The statistical analysis performed for each dataset is indicated in each figure legend.

SUPPLEMENTAL INFORMATION

Supplemental Information includes nine figures and four tables and can be found with this article online at https://doi.org/10.1016/j.ymthe.2017.12.019.

AUTHOR CONTRIBUTIONS

P.V., S.P., P.C., H.C.V., L.J., M.G., F.P., S.M., F.C., M.S.S., S.C., L.v.W., A.V., B.G., and G.R. contributed to the execution of the experiments and data analysis. P.V., S.P., P.C., S.L., I.R., P.L., E.M., G.M., F.R., G.P.C., G.R., and F.M. contributed to the interpretation of results and provided critical insights into the significance of the work. G.R. and F.M. directed the study and wrote the manuscript.

CONFLICTS OF INTEREST

P.V., G.R., and F.M. are inventors in patents describing the treatment of GSDIII disease with dual AAV vectors. All other authors declare no conflicts of interest.

ACKNOWLEDGMENTS

The authors thankfully acknowledge Sarah Wells and the International Mouse Phenotyping Consortium (IMPC) for providing the GSDIII mouse model. We also thank Guy Brochier, Mai Thao, Angeline Madelaine, and Clemence Labasse from the Neuromuscular Histopathology Unit of the Myology Institute for their skillful technical assistance. This work was supported by Genethon and the French Muscular Dystrophy Association (AFM). It was also supported by the European Union's research and innovation program under grant agreements 667751 (MYOCURE to F.M.) and 658712 (GLYCODIS3 to F.M. and G.R.) and the ASTRE laboratories of the Essonne general council grant (to F.M.). The financial support of Italian Telethon is gratefully acknowledged (grant GGP15051 to G.P.C.).

REFERENCES

1. Dagli, A., Sentner, C.P., and Weinstein, D.A. (2010). Glycogen Storage Disease Type III. In GeneReviews, M.P. Adam, H.H. Ardinger, R.A. Pagon, and S.E. Wallace, eds. (Seattle, WA: University of Washington, Seattle).
2. Sentner, C.P., Hoogeveen, I.J., Weinstein, D.A., Santer, R., Murphy, E., McKiernan, P.J., Steuerwald, U., Beauchamp, N.J., Taybert, J., Laforêt, P., et al. (2016). Glycogen storage disease type III: diagnosis, genotype, management, clinical course and outcome. J. Inherit. Metab. Dis. *39*, 697–704.
3. Di Mauro, S.H.A., and Tsujino, S. (2004). Metabolic disorders affecting muscle. In Myology (New York: McGraw-Hill), pp. 1535–1558.
4. Lucchiari, S., Santoro, D., Pagliarani, S., and Comi, G.P. (2007). Clinical, biochemical and genetic features of glycogen debranching enzyme deficiency. Acta Myol. *26*, 72–74.
5. Borowitz, S.M., and Greene, H.L. (1987). Cornstarch therapy in a patient with type III glycogen storage disease. J. Pediatr. Gastroenterol. Nutr. *6*, 631–634.
6. Valayannopoulos, V., Bajolle, F., Arnoux, J.B., Dubois, S., Sannier, N., Baussan, C., Petit, F., Labrune, P., Rabier, D., Ottolenghi, C., et al. (2011). Successful treatment of severe cardiomyopathy in glycogen storage disease type III With D,L-3-hydroxybutyrate, ketogenic and high-protein diet. Pediatr. Res. *70*, 638–641.
7. Dagli, A.I., Zori, R.T., McCune, H., Ivsic, T., Maisenbacher, M.K., and Weinstein, D.A. (2009). Reversal of glycogen storage disease type IIIa-related cardiomyopathy with modification of diet. J. Inherit. Metab. Dis. *32* (*Suppl 1*), S103–S106.
8. Mingozzi, F., and High, K.A. (2011). Therapeutic in vivo gene transfer for genetic disease using AAV: progress and challenges. Nat. Rev. Genet. *12*, 341–355.
9. Nathwani, A.C., Reiss, U.M., Tuddenham, E.G., Rosales, C., Chowdary, P., McIntosh, J., Della Peruta, M., Lheriteau, E., Patel, N., Raj, D., et al. (2014). Long-term safety and efficacy of factor IX gene therapy in hemophilia B. N. Engl. J. Med. *371*, 1994–2004.
10. Maguire, A.M., Simonelli, F., Pierce, E.A., Pugh, E.N., Jr., Mingozzi, F., Bennicelli, J., Banfi, S., Marshall, K.A., Testa, F., Surace, E.M., et al. (2008). Safety and efficacy of gene transfer for Leber's congenital amaurosis. N. Engl. J. Med. *358*, 2240–2248.
11. Mendell, J., Al-Zaidy, S.A., Shell, R., Arnold, W.D., Rodino-Klapac, L.R., Prior, T.W., Lowes, L., Alfano, L.N., Berry, K., Church, K., et al. (2017). AVXS-101 Phase 1 Gene Therapy Clinical Trial in SMA Type 1: Event Free Survival and Achievement of Developmental Milestones. Neurology *88*, CT.003.
12. Mack, D.L., Poulard, K., Goddard, M.A., Latournerie, V., Snyder, J.M., Grange, R.W., Elverman, M.R., Denard, J., Veron, P., Buscara, L., et al. (2017). Systemic AAV8-Mediated Gene Therapy Drives Whole-Body Correction of Myotubular Myopathy in Dogs. Mol. Ther. *25*, 839–854.
13. Yue, Y., Pan, X., Hakim, C.H., Kodippili, K., Zhang, K., Shin, J.H., Yang, H.T., McDonald, T., and Duan, D. (2015). Safe and bodywide muscle transduction in young adult Duchenne muscular dystrophy dogs with adeno-associated virus. Hum. Mol. Genet. *24*, 5880–5890.
14. Pryadkina, M., Lostal, W., Bourg, N., Charton, K., Roudaut, C., Hirsch, M.L., and Richard, I. (2015). A comparison of AAV strategies distinguishes overlapping vectors for efficient systemic delivery of the 6.2 kb Dysferlin coding sequence. Mol. Ther. Methods Clin. Dev. *2*, 15009.
15. Trapani, I., Colella, P., Sommella, A., Iodice, C., Cesi, G., de Simone, S., Marrocco, E., Rossi, S., Giunti, M., Palfi, A., et al. (2014). Effective delivery of large genes to the retina by dual AAV vectors. EMBO Mol. Med. *6*, 194–211.
16. Ghosh, A., Yue, Y., and Duan, D. (2011). Efficient transgene reconstitution with hybrid dual AAV vectors carrying the minimized bridging sequences. Hum. Gene Ther. *22*, 77–83.
17. Raben, N., Plotz, P., and Byrne, B.J. (2002). Acid alpha-glucosidase deficiency (glycogenosis type II, Pompe disease). Curr. Mol. Med. *2*, 145–166.
18. Sun, B., Fredrickson, K., Austin, S., Tolun, A.A., Thurberg, B.L., Kraus, W.E., Bali, D., Chen, Y.T., and Kishnani, P.S. (2013). Alglucosidase alfa enzyme replacement therapy as a therapeutic approach for glycogen storage disease type III. Mol. Genet. Metab. *108*, 145–147.
19. Puzzo, F., Colella, P., Biferi, M.G., Bali, D., Paulk, N.K., Vidal, P., Collaud, F., Simon-Sola, M., Charles, S., Hardet, R., et al. (2017). Rescue of Pompe disease in mice by AAV-mediated liver delivery of secretable acid α-glucosidase. Sci. Transl. Med. *9*, eaam6375.

20. Ghosh, A., Yue, Y., Lai, Y., and Duan, D. (2008). A hybrid vector system expands adeno-associated viral vector packaging capacity in a transgene-independent manner. Mol. Ther. *16*, 124–130.

21. Ronzitti, G., Bortolussi, G., van Dijk, R., Collaud, F., Charles, S., Leborgne, C., Vidal, P., Martin, S., Gjata, B., Sola, M.S., et al. (2016). A translationally optimized AAV-UGT1A1 vector drives safe and long-lasting correction of Crigler-Najjar syndrome. Mol. Ther. Methods Clin. Dev. *3*, 16049.

22. Rabinowitz, J.E., Rolling, F., Li, C., Conrath, H., Xiao, W., Xiao, X., and Samulski, R.J. (2002). Cross-packaging of a single adeno-associated virus (AAV) type 2 vector genome into multiple AAV serotypes enables transduction with broad specificity. J. Virol. *76*, 791–801.

23. Löser, P., Jennings, G.S., Strauss, M., and Sandig, V. (1998). Reactivation of the previously silenced cytomegalovirus major immediate-early promoter in the mouse liver: involvement of NFkappaB. J. Virol. *72*, 180–190.

24. Miao, C.H., Ohashi, K., Patijn, G.A., Meuse, L., Ye, X., Thompson, A.R., and Kay, M.A. (2000). Inclusion of the hepatic locus control region, an intron, and untranslated region increases and stabilizes hepatic factor IX gene expression in vivo but not in vitro. Mol. Ther. *1*, 522–532.

25. Gao, G.P., Alvira, M.R., Wang, L., Calcedo, R., Johnston, J., and Wilson, J.M. (2002). Novel adeno-associated viruses from rhesus monkeys as vectors for human gene therapy. Proc. Natl. Acad. Sci. USA *99*, 11854–11859.

26. Huijing, F. (1975). Glycogen metabolism and glycogen-storage diseases. Physiol. Rev. *55*, 609–658.

27. Yi, H., Brooks, E.D., Thurberg, B.L., Fyfe, J.C., Kishnani, P.S., and Sun, B. (2014). Correction of glycogen storage disease type III with rapamycin in a canine model. J. Mol. Med. (Berl.) *92*, 641–650.

28. Mayorandan, S., Meyer, U., Hartmann, H., and Das, A.M. (2014). Glycogen storage disease type III: modified Atkins diet improves myopathy. Orphanet J. Rare Dis. *9*, 196.

29. Brambilla, A., Mannarino, S., Pretese, R., Gasperini, S., Galimberti, C., and Parini, R. (2014). Improvement of Cardiomyopathy After High-Fat Diet in Two Siblings with Glycogen Storage Disease Type III. JIMD Rep. *17*, 91–95.

30. Derks, T.G., and Smit, G.P. (2015). Dietary management in glycogen storage disease type III: what is the evidence? J. Inherit. Metab. Dis. *38*, 545–550.

31. Yi, H., Zhang, Q., Brooks, E.D., Yang, C., Thurberg, B.L., Kishnani, P.S., and Sun, B. (2017). Systemic Correction of Murine Glycogen Storage Disease Type IV by an AAV-Mediated Gene Therapy. Hum. Gene Ther. *28*, 286–294.

32. Zhai, L., Feng, L., Xia, L., Yin, H., and Xiang, S. (2016). Crystal structure of glycogen debranching enzyme and insights into its catalysis and disease-causing mutations. Nat. Commun. *7*, 11229.

33. Ferla, R., Claudiani, P., Cotugno, G., Saccone, P., De Leonibus, E., and Auricchio, A. (2014). Similar therapeutic efficacy between a single administration of gene therapy and multiple administrations of recombinant enzyme in a mouse model of lysosomal storage disease. Hum. Gene Ther. *25*, 609–618.

34. Ruzo, A., Garcia, M., Ribera, A., Villacampa, P., Haurigot, V., Marco, S., Ayuso, E., Anguela, X.M., Roca, C., Agudo, J., et al. (2012). Liver production of sulfamidase reverses peripheral and ameliorates CNS pathology in mucopolysaccharidosis IIIA mice. Mol. Ther. *20*, 254–266.

35. Trapani, I., Toriello, E., de Simone, S., Colella, P., Iodice, C., Polishchuk, E.V., Sommella, A., Colecchi, L., Rossi, S., Simonelli, F., et al. (2015). Improved dual AAV vectors with reduced expression of truncated proteins are safe and effective in the retina of a mouse model of Stargardt disease. Hum. Mol. Genet. *24*, 6811–6825.

36. Austin, S.L., Proia, A.D., Spencer-Manzon, M.J., Butany, J., Wechsler, S.B., and Kishnani, P.S. (2012). Cardiac Pathology in Glycogen Storage Disease Type III. JIMD Rep. *6*, 65–72.

37. Barzel, A., Paulk, N.K., Shi, Y., Huang, Y., Chu, K., Zhang, F., Valdmanis, P.N., Spector, L.P., Porteus, M.H., Gaensler, K.M., and Kay, M.A. (2015). Promoterless gene targeting without nucleases ameliorates haemophilia B in mice. Nature *517*, 360–364.

38. Li, H., Haurigot, V., Doyon, Y., Li, T., Wong, S.Y., Bhagwat, A.S., Malani, N., Anguela, X.M., Sharma, R., Ivanciu, L., et al. (2011). In vivo genome editing restores haemostasis in a mouse model of haemophilia. Nature *475*, 217–221.

39. Demo, E., Frush, D., Gottfried, M., Koepke, J., Boney, A., Bali, D., Chen, Y.T., and Kishnani, P.S. (2007). Glycogen storage disease type III-hepatocellular carcinoma a long-term complication? J. Hepatol. *46*, 492–498.

40. Mingozzi, F., Hasbrouck, N.C., Basner-Tschakarjan, E., Edmonson, S.A., Hui, D.J., Sabatino, D.E., Zhou, S., Wright, J.F., Jiang, H., Pierce, G.F., et al. (2007). Modulation of tolerance to the transgene product in a nonhuman primate model of AAV-mediated gene transfer to liver. Blood *110*, 2334–2341.

41. Fields, P.A., Arruda, V.R., Armstrong, E., Chu, K., Mingozzi, F., Hagstrom, J.N., Herzog, R.W., and High, K.A. (2001). Risk and prevention of anti-factor IX formation in AAV-mediated gene transfer in the context of a large deletion of F9. Mol. Ther. *4*, 201–210.

42. Chuah, M.K., Petrus, I., De Bleser, P., Le Guiner, C., Gernoux, G., Adjali, O., Nair, N., Willems, J., Evens, H., Rincon, M.Y., et al. (2014). Liver-specific transcriptional modules identified by genome-wide in silico analysis enable efficient gene therapy in mice and non-human primates. Mol. Ther. *22*, 1605–1613.

43. Liu, Y.L., Mingozzi, F., Rodriguéz-Colôn, S.M., Joseph, S., Dobrzynski, E., Suzuki, T., High, K.A., and Herzog, R.W. (2004). Therapeutic levels of factor IX expression using a muscle-specific promoter and adeno-associated virus serotype 1 vector. Hum. Gene Ther. *15*, 783–792.

44. Duan, D. (2016). Systemic delivery of adeno-associated viral vectors. Curr. Opin. Virol. *21*, 16–25.

45. Le Guiner, C., Montus, M., Servais, L., Cherel, Y., Francois, V., Thibaud, J.L., Wary, C., Matot, B., Larcher, T., Guigand, L., et al. (2014). Forelimb treatment in a large cohort of dystrophic dogs supports delivery of a recombinant AAV for exon skipping in Duchenne patients. Mol. Ther. *22*, 1923–1935.

46. Sondergaard, P.C., Griffin, D.A., Pozsgai, E.R., Johnson, R.W., Grose, W.E., Heller, K.N., Shontz, K.M., Montgomery, C.L., Liu, J., Clark, K.R., et al. (2015). AAV.Dysferlin Overlap Vectors Restore Function in Dysferlinopathy Animal Models. Ann. Clin. Transl. Neurol. *2*, 256–270.

47. Koo, T., Popplewell, L., Athanasopoulos, T., and Dickson, G. (2014). Triple trans-splicing adeno-associated virus vectors capable of transferring the coding sequence for full-length dystrophin protein into dystrophic mice. Hum. Gene Ther. *25*, 98–108.

48. Lostal, W., Bartoli, M., Bourg, N., Roudaut, C., Bentaïb, A., Miyake, K., Guerchet, N., Fougerousse, F., McNeil, P., and Richard, I. (2010). Efficient recovery of dysferlin deficiency by dual adeno-associated vector-mediated gene transfer. Hum. Mol. Genet. *19*, 1897–1907.

49. Mendell, J.R. (2016). rAAVrh74.MHCK7.DYSF.DV for treatment of dysferlinopathies. https://clinicaltrials.gov/ct2/show/NCT02710500.

50. Hers, H.G., Verhue, W., and Van hoof, F. (1967). The determination of amylo-1,6-glucosidase. Eur. J. Biochem. *2*, 257–264.

51. Zhang, P., Sun, B., Osada, T., Rodriguiz, R., Yang, X.Y., Luo, X., Kemper, A.R., Clay, T.M., and Koeberl, D.D. (2012). Immunodominant liver-specific expression suppresses transgene-directed immune responses in murine pompe disease. Hum. Gene Ther. *23*, 460–472.

52. Sun, B., Zhang, H., Franco, L.M., Young, S.P., Schneider, A., Bird, A., Amalfitano, A., Chen, Y.T., and Koeberl, D.D. (2005). Efficacy of an adeno-associated virus 8-pseudotyped vector in glycogen storage disease type II. Mol. Ther. *11*, 57–65.

53. Matsushita, T., Elliger, S., Elliger, C., Podsakoff, G., Villarreal, L., Kurtzman, G.J., Iwaki, Y., and Colosi, P. (1998). Adeno-associated virus vectors can be efficiently produced without helper virus. Gene Ther. *5*, 938–945.

54. Ayuso, E., Mingozzi, F., Montane, J., Leon, X., Anguela, X.M., Haurigot, V., Edmonson, S.A., Africa, L., Zhou, S., High, K.A., et al. (2010). High AAV vector purity results in serotype- and tissue-independent enhancement of transduction efficiency. Gene Ther. *17*, 503–510.